

## Seasonal nearshore sediment resuspension and water clarity at Lake Tahoe

Kristin E. Reardon, Patricio A. Moreno-Casas, Fabián A. Bombardelli & S. Geoffrey Schladow

To cite this article: Kristin E. Reardon, Patricio A. Moreno-Casas, Fabián A. Bombardelli & S. Geoffrey Schladow (2016) Seasonal nearshore sediment resuspension and water clarity at Lake Tahoe, Lake and Reservoir Management, 32:2, 132-145, DOI: [10.1080/10402381.2015.1136013](https://doi.org/10.1080/10402381.2015.1136013)

To link to this article: <http://dx.doi.org/10.1080/10402381.2015.1136013>



Published online: 02 Mar 2016.



Submit your article to this journal [↗](#)



View related articles [↗](#)



View Crossmark data [↗](#)

## Seasonal nearshore sediment resuspension and water clarity at Lake Tahoe

Kristin E. Reardon<sup>a,b,c</sup>, Patricio A. Moreno-Casas<sup>a,d</sup>, Fabián A. Bombardelli<sup>a</sup>, and S. Geoffrey Schladow<sup>a,b</sup>

<sup>a</sup>Department of Civil and Environmental Engineering, University of California, Davis, 2001 Ghausi Hall, One Shields Avenue, Davis, CA; <sup>b</sup>Tahoe Environmental Research Center, University of California, Davis, 291 Country Club Drive, Incline Village, NV; <sup>c</sup>CH2M, 949 East Thirty-sixth Avenue, Anchorage, AK; <sup>d</sup>Facultad de Ingeniería y Ciencias Aplicadas, Universidad de los Andes, Mons. Álvaro del Portillo 12455, Las Condes, Santiago, Chile

### ABSTRACT

Reardon KE, Moreno-Casas PA, Bombardelli FA, Schladow SG. 2016 Seasonal nearshore sediment resuspension and water clarity at Lake Tahoe. *Lake Reserv Manage.* 32:132–145.

Motivated by management challenges due to declining water clarity at Lake Tahoe, California–Nevada, we synthesized field observations and modeling of wind-driven nearshore sediment resuspension to inform decision-makers. We present the first field observations of nearshore sediment resuspension in both summer and winter and investigate seasonal differences in lake behavior. In addition, using a previously modified and validated wind-wave model, STWAVE, we developed management charts that illustrate relationships between fetch, wind intensity, and wave height and between water depth, wave height, and the potential for mobilization of different-sized particles. For a representative grain size of 150  $\mu\text{m}$ , the wind-driven surface waves were found to influence the sediments to a maximum water depth of 9 m. Additionally, we evaluated the potential for wind-driven nearshore sediment resuspension with changing lake levels, considering a range of possible future scenarios. The areal extent of potential wind-driven sediment resuspension in Lake Tahoe's southern nearshore zone is maximum (8.3 km<sup>2</sup>) at a lake water level equal to the natural rim (1897 m). The potential for resuspension notwithstanding, the results demonstrated no increase in particle loading of the size class identified to most negatively impact water clarity (<16  $\mu\text{m}$ ). Therefore, we corroborate previous findings and conclude that wind-driven nearshore sediment resuspension does not contribute to the declining water clarity of Lake Tahoe and attribute this to a lack of available fine material within the lake sediments.

### KEY WORDS

Lake Tahoe; nearshore sediment resuspension; STWAVE; water clarity; wind-waves

We typically assume that disturbances at the sediment–water interface negatively influence lake clarity. Particulates and nutrients may be present in the water column; they may enter a waterbody from diverse external sources; or they may be reintroduced from within the system itself, such as when previously deposited sediments are resuspended from the sediment bed. The general concept of sediment resuspension is predicated on the comparison of a destabilizing parameter (e.g., bottom shear stress) with a critical condition (e.g., the critical shear stress for a representative grain size; Parker 2004, García 2008). In keeping with standard practice, we too reason that sediment resuspension occurs when the destabilizing parameter exceeds the critical condition by a certain value. Wind-driven sediment resuspension takes place when the water depth is shallow enough to favor the transfer of sufficient momentum of the wind-waves

from the water surface to the sediment–water interface (Håkanson and Jansson 1983, Kundu et al. 2012). Therefore, in an otherwise deep lake, only the shallow nearshore zone is susceptible to wind-driven sediment resuspension, in contrast to a shallow lake where wind-driven sediment resuspension may occur over the entire areal extent of the lake (Luettich et al. 1990, Chung et al. 2009a, 2009b).

Lake Tahoe is a deep, subalpine lake with remarkably transparent waters. Nevertheless, lake transparency has declined since long-term monitoring began in the 1960s. In 1982, Lake Tahoe was designated an impaired waterbody by the US Environmental Protection Agency. Under the Federal Clean Water Act, a total maximum daily load (TMDL) was required to address its impairment. The agreed-upon water quality objective for Lake Tahoe is deep water transparency equal to the average annual Secchi depth measured

between 1967 and 1971 (29.7 m). The Lake Tahoe TMDL identifies the pollutants responsible for the loss of transparency as fine sediment ( $<16 \mu\text{m}$ ), nitrogen, and phosphorus (California Regional Water Quality Control Board, Lahontan Region and Nevada Division of Environmental Protection 2010). The Lake Tahoe TMDL also identifies the load of each pollutant entering the lake, the contributing sources of these loads, the reductions needed, the reduction opportunities available for each source, and the implementation plan to achieve these reductions (California Regional Water Quality Control Board, Lahontan Region and Nevada Division of Environmental Protection 2010). Until now, a comprehensive investigation of the potential for internal sources of fine sediment (i.e., resuspended sediment) has been lacking, yet at other wind-exposed lakes, sediment resuspension can be a significant source of fine sediment (Evans 1994, Bloesch 1994, Chung et al. 2009a, 2009b).

Reardon et al. (2014) investigated wind-driven nearshore sediment resuspension at Lake Tahoe in winter and found instances of wind-driven sediment resuspension as corroborated by simultaneous increases in bottom shear stress and total measured suspended sediment concentration (SSC). In that study, the authors developed a novel methodology to directly estimate total bottom shear stress by its contributions from wind-waves, mean currents, and random motions and found that the total shear stress exceeding the critical shear stress was due to the overwhelming contribution of wind-waves (80%). In addition, the authors successfully extended and validated modifications to the US Army Corps of Engineers (USACE) wind-wave model STWAVE to simulate wind-driven sediment resuspension for viscous-dominated flow typical in lakes. Previously, lake applications of STWAVE had been limited to special instances of fully turbulent flow as a result of hurricane conditions (Bunya et al. 2010, Dietrich et al. 2010); in these cases, bottom-friction was accounted for using Manning's equation, which was appropriate for fully turbulent flow. To accommodate a viscous-dominated flow, Reardon et al. (2014) introduced a key change to the STWAVE subroutine (friction) whereby the bottom friction coefficient was estimated with the expression from Kamphuis (1975) for viscous-dominated conditions. This modification was necessary because the field data showed that lake flow near the bed was viscous-dominated with a wave Reynolds number  $<10^4$ . Lastly, Reardon et al. (2014) presented and analyzed *in situ*

measurements of SSC and particle size distribution for several instances of low-wind and high-wind periods; for those periods, the concentration of fine sediment in suspension remained unchanged. Therefore, we concluded that further consideration of winter and summer conditions was warranted because we could no longer presume that wind-driven disturbances at the sediment–water interface contributed to an increase in the fine-sediment load responsible for Lake Tahoe's declining water clarity.

Also of interest were the potential implications of climate change with changing water level and/or wind intensity. Water level at Lake Tahoe over the next century is projected to vary within the range we have identified for our model runs (Sahoo et al. 2012). The range extends from a water surface elevation 2 m below the natural rim (1895 m) up to the maximum legal limit (1899 m; all referenced to NAVD 88). Also in the Tahoe Basin, wind speed is projected to decrease 4–5% over the next century relative to historical averages (Dettinger 2012).

To investigate nearshore sediment resuspension and consider seasonal differences in such phenomenon, we synthesized field observations of hydrodynamic and sediment variables, computations of bottom shear stress from field data, and simulations from a previously modified and validated wind-wave model with the aim of answering the following questions:

1. What are the differences in resuspension events between summer and winter in Lake Tahoe? How does bottom shear stress change from one season to another?
2. Because the surface layers of lakes experience warming, does the temperature difference affect the water column dynamics and in turn sediment resuspension?
3. To what water depth do wind-driven surface waves influence the sediments?
4. What lake area does this influence extend, and how does it change with changing lake level?
5. What are the implications of wind-driven nearshore sediment resuspension for water quality at Lake Tahoe during different times of the year?

## Study site

Lake Tahoe, located in the western United States on the California–Nevada border in the mountains of the Sierra Nevada (Fig. 1), is an example of a deep, olig-

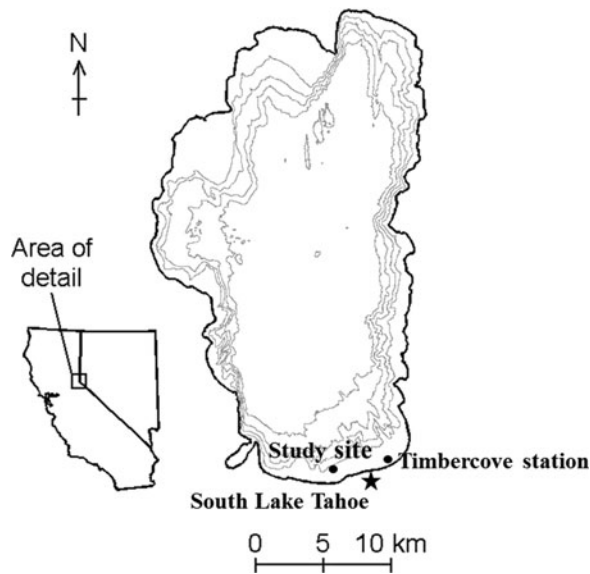


**Figure 1.** Lake Tahoe ( $\sim 39^\circ\text{N}$ ,  $120^\circ\text{W}$ ) bathymetry and orientation. Meteorological data were collected at Timbercove station, and lake measurements were collected at the study site. Contours are shown at 100 m intervals.

otrophic lake as characterized by low nutrient concentrations, high dissolved oxygen concentrations, and exceptionally transparent water to great depths. Lake Tahoe is large within a small watershed and has an extremely long hydraulic residence time (Table 1).

The nearshore study site was located at the south end of Lake Tahoe 1000 m offshore on a shallow, broad, gently sloping shelf ( $\sim 0.3\%$ ; Fig. 1). We collected meteorological data from the long-term meteorological station maintained by the University of California, Davis, Tahoe Environmental Research Center (TERC) on the pier at Timbercove near the City of South Lake Tahoe. Timbercove station, the nearest long-term meteorological station, was located 4.5 km from the study site (Fig. 1).

**Table 1.** Lake Tahoe summary information.

Maximum depth	505 m
Average depth	313 m
Lake surface area	500 km <sup>2</sup>
Watershed area	800 km <sup>2</sup>
Lake volume	156 km <sup>3</sup>
Shoreline	116 km
Mean hydraulic residence time	700 yr
Elevation of natural rim <sup>a</sup>	1897 m
Elevation of maximum legal limit <sup>a, b</sup>	1899 m
Annual average Secchi depth (target) <sup>c</sup>	29.7 m
Annual average Secchi depth (2014) <sup>d</sup>	23.7 m

<sup>a</sup>Referenced to NAVD 88.

<sup>b</sup>Fixed according to the Truckee River Operating Agreement (<https://troa.net/>).

<sup>c</sup>From California Regional Water Quality Control Board, Lahontan Region and Nevada Division of Environmental Protection (2010).

<sup>d</sup>From UCD TERC (2015).

All other information from Goldman (1988).

## Methods

### Field observations and computations from field data

We took lake measurements in summer from 22 July to 3 September 2008 and in winter from 13 November 2008 to 14 January 2009 with a total water depth varying between 4.5 and 5 m. We measured vertical profiles of water temperature with a thermistor chain of 8 Onset Stow Away TidbiT temperature loggers. We measured nearbed velocity with 2 acoustic Doppler velocimeters (ADV), a Nortek Vector, and a Sontek ADVOcean Probe, mounted on a sawhorse frame. We measured nearbed SSC and particle size distribution with a Laser In Situ Scattering and Transmissometry 100X Type B instrument (LISST-100X) from Sequoia Scientific, Inc. The LISST-100X was deployed on 2 aluminum risers about 2 m from the sawhorse frame; the raw data were processed and converted according to Andrews et al. (2011). We characterized lakebed sediment from 2 grab samples processed using an LS 13 320 MW particle-size analyzer from Beckman Coulter, Inc. All field data were collected at the study site with the exception of wind data. We measured wind speed and direction 5 m above lake level at Timbercove station.

Instrument sampling strategies in summer and winter were the same (and at the same location) with 2 exceptions. Lakebed sediment characteristics were determined from grab samples collected solely in summer (22 Jul 2008). We assumed that lakebed sediment characteristics did not change from summer to winter, a reasonable assumption considering our visual estimation of the study site, the relatively small contribution to the lake by the inflow streams, and the continuous absence of bedforms. Measurements of SSC and particle size distribution were collected solely in winter (11 Dec 2008 to 14 Jan 2009). Field measurements including the parameter(s) measured, instrument, sampling period, sampling interval, sampling duration, and burst interval, as applicable, were summarized (Table 2).

In addition to measurements collected during the 2 study periods, we analyzed 10 years of wind data collected at Timbercove station from 1 June 2003 to 31 July 2013 to characterize the seasonal wind exposure at the study site (Table 2). We define summer as June through September and winter as December through March.

**Table 2.** Field measurements for Lake Tahoe in summer and winter.

Parameter(s) measured	Instrument	Sampling period		Sampling frequency		
		Summer	Winter	Interval	Duration	Burst interval
Wind speed and direction <sup>a</sup>	Met One Windset 3-cup anemometer	ongoing	ongoing	10 min	NA	NA
Vertical profiles of water temperature <sup>b</sup>	Onset Stow Away TidbiT temperature loggers	23 Jul–3 Sep	13 Nov–14 Jan	5 min	NA	NA
Nearbed velocity <sup>c,d</sup>	Sontek ADVOcean Probe	23 Jul–29 Aug	13 Nov–21 Dec	10 Hz	3 min	1 h
Nearbed velocity <sup>c,e</sup>	Nortek Vector	23 Jul–27 Aug	13 Nov–19 Dec	64 Hz	2 min	2 h
SSC and particle size distribution <sup>c,e</sup>	LISST-100X	NA	11 Dec–14 Jan	1 Hz	2 min	2 h
Lakebed sediment characteristics	Grab samples (2)	22 Jul	NA	NA	NA	NA

<sup>a</sup>Wind speed and direction were measured at Timbercove station located at N38°56.99', W119°58.07'.

<sup>b</sup>Eight temperature loggers were positioned at heights of 0.2, 0.5, 1.0, 1.5, 2.0, 2.5, 3.0, and 3.5 m above lakebed and located at N38°56.57', W120°1.18'.

<sup>c</sup>Located at N38°56.46', W120°1.17'.

<sup>d</sup>Sampling volume was 0.10 m above lakebed.

<sup>e</sup>Sampling volume was 0.20 m above lakebed.

NA = not applicable.

We directly estimated bottom shear stress from ADV-measured velocity data collected from the Sontek ADVOcean Probe. According to the method developed in Reardon et al. (2014), we partitioned bottom shear stress into 3 components attributed to wind-waves, mean currents, and random motions by filtering the vertical component of the velocity for each high-frequency burst and considering its fluctuations as a variation of the turbulent kinetic energy method from Kim et al. (2000). Using a second-order Butterworth filter and applying a band-pass filter that passed all frequencies between 0.03 and 2 Hz, a low-pass filter that passed all frequencies below 0.03 Hz, and a high-pass filter that passed all frequencies above 2 Hz, we separated the vertical component of the velocity into 3 contributing parts attributed to wind-waves, mean currents, and random motions, respectively. Reardon et al. (2014) demonstrated that with increasing total bottom shear stress, the relative contribution of each component became distinct due to the overwhelming contribution of wind-waves (80%).

To compute the value of critical shear stress, we used the formulation from Parker (2004) that incorporates the nondimensional critical Shields parameter. The Shields diagram (Shields 1936) for threshold of sediment particle motion in unidirectional, steady, uniform flow adequately characterizes incipient conditions under oscillatory flows (Raudkivi 1998, Chung et al. 2009a). This is a reasonable approach considering the surface wavefield of wind-exposed lakes.

### Wind-wave modeling

To estimate the wind-wave contribution to bottom shear stress, we implemented a previously modified and validated form of the full-plane version of the USACE wind-wave model STWAVE (see Reardon et al. 2014). STWAVE is a finite difference, steady-state, spectral wave model that solves the wave action balance equation, including wave generation and transformation by refraction and shoaling, wave breaking, generation by wind-input, wave-wave interaction, and white-capping (Massey et al. 2011). Reardon et al. (2014) modified the bottom-friction formulation within the code to reflect typical lake conditions with flow regimes that were viscous-dominated. Earlier lake applications of STWAVE had been limited to special instances of fully turbulent flow as a result of hurricane conditions (e.g., Bunya et al. 2010, Dietrich et al. 2010). The modified STWAVE was validated and is an appropriate tool to calculate the effect of wind-waves on the development of bottom shear stress leading to sediment resuspension in the shallow nearshore area of a deep lake (Reardon et al. 2014).

We implemented the modified STWAVE lake-wide using 50 m square grid cells to which we specified bathymetry. The bathymetry data were prepared by merging US Geological Survey multibeam sonar and USACE SCHOALS bathymetry datasets, both with a grid spacing of 10 m (T.E. Steissberg, University of California, Davis, 2009, unpubl. data). We used the modified STWAVE to consider a range of wind conditions and the resulting bottom sediment dynamics. We based

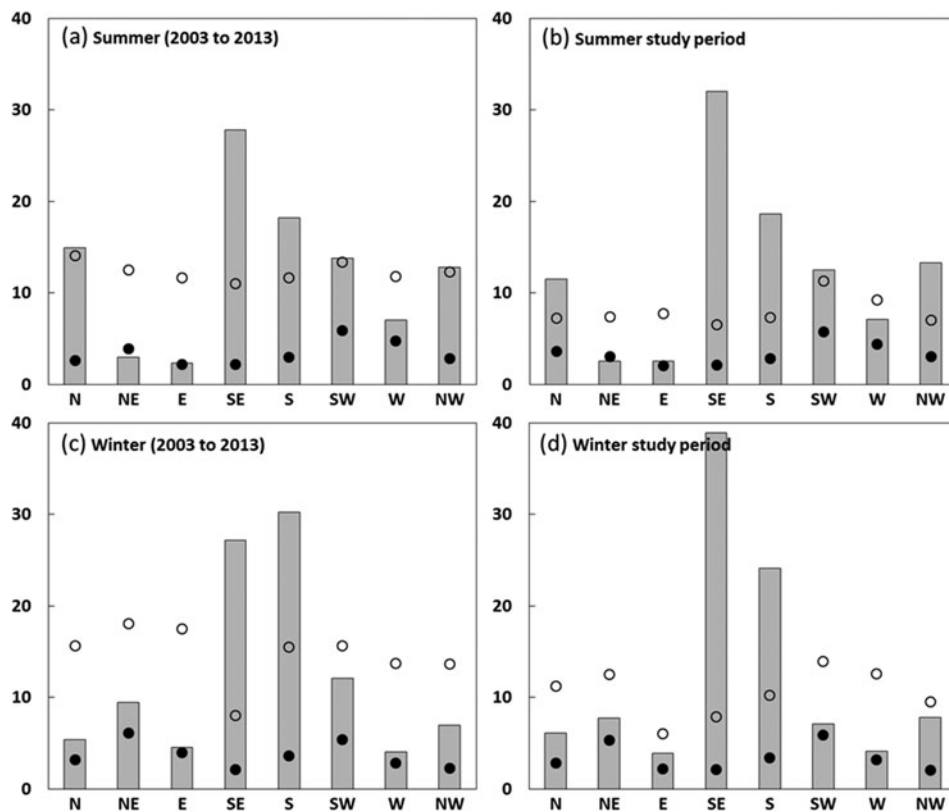


**Figure 2.** Wind statistics separated by wind direction at Timbercove station for (a) summer 2003–2013, (b) summer during the study period, (c) winter 2003–2013, and (d) winter during the study period. Bars represent percent of wind data separated by wind direction. Wind speeds (m/s) are given as mean (closed circle) and maximum (open circle).

our analysis on the work of Norrman (1964), who presented relationships between wave height, wind conditions, effective fetch, and sediment response at Lake Vättern (Sweden; Håkanson and Jansson 1983). Using the modified STWAVE, we developed similar relationships based on Lake Tahoe and suggest that other lakes could be likewise considered.

In particular, we reproduced wind events ranging from 3 to 21 m/s coming from different directions. Seven wind velocities (3, 6, 9, 12, 15, 18, and 21 m/s) and 5 wind directions (0, 30, 45, 60, and 90, degrees measured clockwise from north) represented a range of realistic wind events at Lake Tahoe. Considering the study site in the southern part of the lake, the longest fetch (~30 km) results from a northerly wind (i.e., a wind direction equal to 0 degrees clockwise from north). Conversely, the shortest fetch (~1 km) results from a southerly wind (i.e., a wind direction equal to 180 degrees clockwise from north). The angles covered a full range of northeasterly winds, which produced a similar effect as corroborated by simulations (not shown). We simulated northerly winds because these have the longest fetch and therefore generate the

greatest resuspension potential for these wind intensities. We implemented 35 simulations in the modified STWAVE and calculated significant wave heights, wave periods, bottom orbital velocities, and bottom shear stresses for each cell, based on wave motions alone, (i.e., neglecting the presence of mean currents). We then used the results of modeled bottom shear stress to calculate the corresponding maximum particle diameter that could be resuspended from the lakebed considering the formulation of critical shear stress. Once we obtained the potential resuspension of the maximum particle diameter for each incremental bottom shear stress, we computed equation coefficients using the multivariate regression tool in the commercially available software package MATLAB. In this way, we developed predictive equations relating wind, water depth, and the potential for mobilization of different-sized particles.

To quantify the areal extent of wind-driven nearshore sediment resuspension at Lake Tahoe with changing lake water level, we ran the modified STWAVE model with water surface elevations between 2 m below the natural rim (1895 m) and the maximum

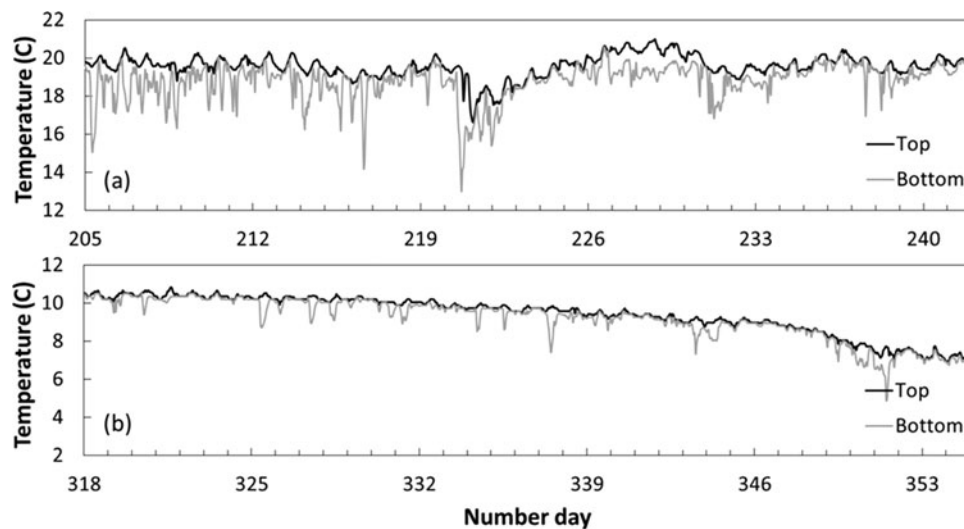


**Figure 3.** Water temperature observed from (a) 23 July to 29 August 2008 (summer) and (b) 13 November to 20 December 2008 (winter) at the study site for top and bottom thermistors. The temperature at the top thermistor remains nearly equal to or greater than that of the bottom thermistor, implying thermodynamic neutrality or stability.

legal limit (1899 m) in increments of 0.5 m (the natural rim of the lake is 1897 m, all referenced to NAVD 88), and for wind speed and direction that generated the maximum shear stress. In this way, we defined an area of maximum potential wind-driven sediment resuspension. Lake level is influenced by stream inflow, groundwater inflow, direct precipitation, evaporation, outflow, and overflow, as applicable, and is therefore affected by climate change. Considering these processes, Sahoo et al. (2012) projected water levels at Lake Tahoe over the next century. Future climate conditions drier than normal will likely result in a water surface elevation below the natural rim; conversely, future climate conditions wetter than normal will likely result in water surface elevations above the natural rim, up to the maximum legal limit.

We did not consider future scenarios for which the wind intensity changes. In general, researchers predict a decrease in wind intensity as average global temperatures increase (Ren 2010). Focusing on the Tahoe Basin in particular, Dettinger (2012) spatially downscaled meteorology output from the coupled ocean-atmosphere general circulation model (CM2.1) of the National Oceanic and Atmospheric Administration's Geophysical Fluid Dynamics Laboratory in response to 2 greenhouse-gas emissions scenarios (A2 and B1). Considering both scenarios for the Tahoe Basin, wind speeds are projected to decrease 4–5% over the next century relative to historical averages (Dettinger 2012); therefore, our consideration of wind intensity from recent meteorological data (2003–2013)

represents our understanding of the greatest potential for wind energy input into the lake. Future scenarios considering decreased wind speeds would result in less potential for nearshore sediment resuspension.

## Results and discussion

### Wind exposure

From the Timbercove wind record from 1 June 2003 to 31 July 2013, we observed predominantly southerly winds (SW, S, SE) representing 60% of the winds over the 10 yr period (not shown) and 60–70% of the winds measured in summer and winter (Fig. 2). Northerly winds (NW, N, NE) represented 22–31% of the wind record measured in summer and winter (Fig. 2).

Averaging over the summer period, the mean wind speed by direction ranged from 2.1 to 5.9 m/s and was most frequently from the southeast direction (Fig. 2a). For the study period, the mean wind speed ranged from 2.0 to 5.7 m/s and was most frequently southeasterly, as observed in daily mid-afternoon peaks (Fig. 2b and 4a). Averaging over the winter period, the mean wind speed by direction ranged from 2.1 to 6.1 m/s, and the greatest mean wind speed was associated with northeasterly winds (Fig. 2c). The greatest value of wind speed over the entire winter record was from the northeast (18.1 m/s; Fig. 2c); the greatest value of wind speed over the winter study period was from the southwest (13.9 m/s; Fig. 2d and 5a). The maximum wind speed observed during the study periods of 2008 and 2009

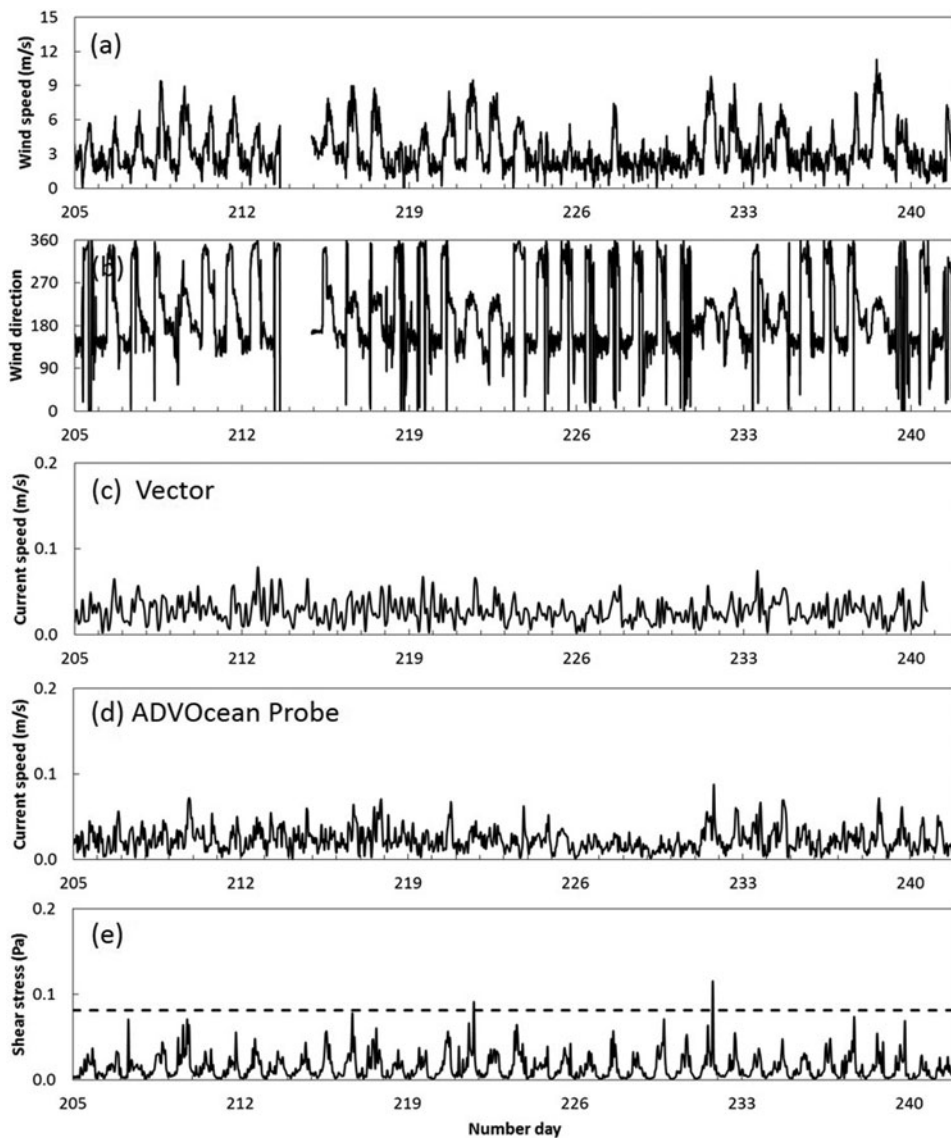


**Figure 4.** Comparison of observed variables in summer from 23 July through 29 August 2008: (a) wind speed and (b) wind direction (degrees clockwise from north) measured at Timbercove station, burst-averaged nearbed current speed in the horizontal plane at (c) 0.20 m (Vector) and (d) 0.10 m (ADVOcean Probe) from the bottom, and (e) total bottom shear stress at a water depth of 5 m computed from data collected by the ADVOcean Probe. The horizontal dashed line at 0.081 Pa indicates the critical shear stress for incipient motion for a representative particle size of 150  $\mu\text{m}$ .

was less than for the 10 yr record; however, the mean wind speed was comparable.

#### **Observed nearshore patterns in summer and winter**

Patterns of physical phenomena were different in summer and winter, as expected. In summer, we observed a reliable diurnal pattern of nearshore water warming and cooling with a daily difference of 2 C (Fig. 3a). In winter, the diurnal pattern was more subtle, and, in general, the temperature of bottom and top thermistors

tracked closely (Fig. 3b). We saw a greater temperature difference between bottom and top thermistors in summer (3 C on average; Fig. 3a) than in winter (1 C on average; Fig. 3b). These temperature differences, however, were usually sustained for 2–4 h and no more than 6 h.

During the summer study period we observed a pattern of daily, elevated, mid-afternoon wind speeds  $>6$  m/s in a south–southeasterly direction. Wind speeds  $\geq 9$  m/s were observed several times in a northerly direction (see Fig. 4a and 4b; days 208–209

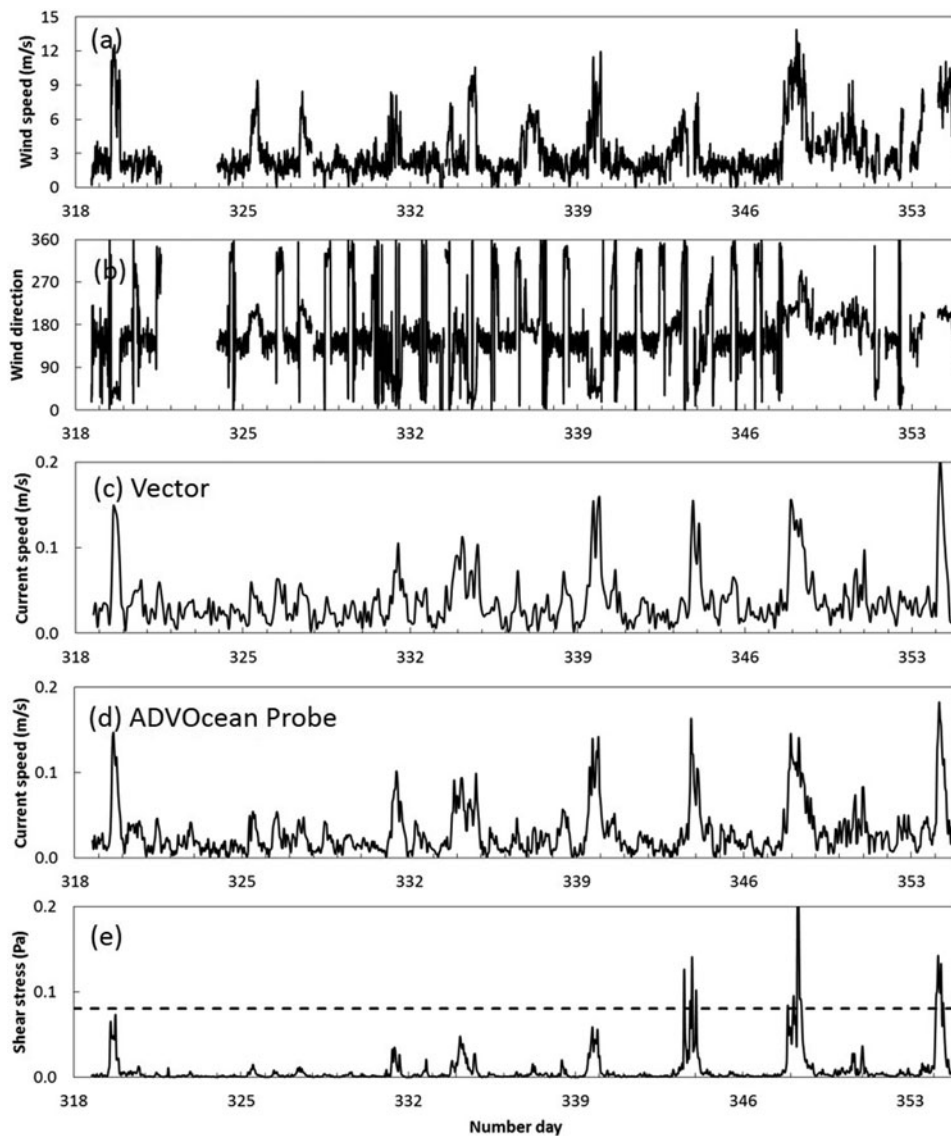


**Figure 5.** Comparison of observed variables in winter from 13 November to 20 December 2008: (a) wind speed and (b) wind direction (degrees clockwise from north) measured at Timbercove station, burst-averaged nearbed current speed in the horizontal plane at (c) 0.20 m (Vector) and (d) 0.10 m (ADVOcean Probe) from the bottom, and (e) total bottom shear stress at a water depth of 5 m computed from data collected by the ADVOcean Probe. The horizontal dashed line at 0.081 Pa indicates the critical shear stress for incipient motion for a representative particle size of  $150\ \mu\text{m}$ .

and 216) and south-southwesterly direction (Fig. 4a and 4b; days 221, 231–232, and 238). For the winter study period, we observed low wind speeds punctuated by high-energy wind events; no regular daily wind patterns were observed in winter (Fig. 5a and 5b).

During the summer study period, we observed an average nearbed current speed of 0.03 m/s measured with the Vector and ADVOcean Probe. Peaks in nearbed current speed were  $<0.10$  m/s (Fig. 4c and 4d), in contrast to winter conditions with nearbed

current speed peaks of 0.15–0.20 m/s (Fig. 5c and 5d).

Spectra from different high-frequency, nearbed velocity bursts collected using the ADVOcean Probe during high-wind events throughout the summer and winter have a significant difference associated with the peaks in energy, yet yield a generally similar form (Fig. 6). The peak of the power spectral density ranged from 0.28 to 0.37 Hz, corresponding to wave periods between 2.7 and 3.2 s. For the 2 summer bursts,

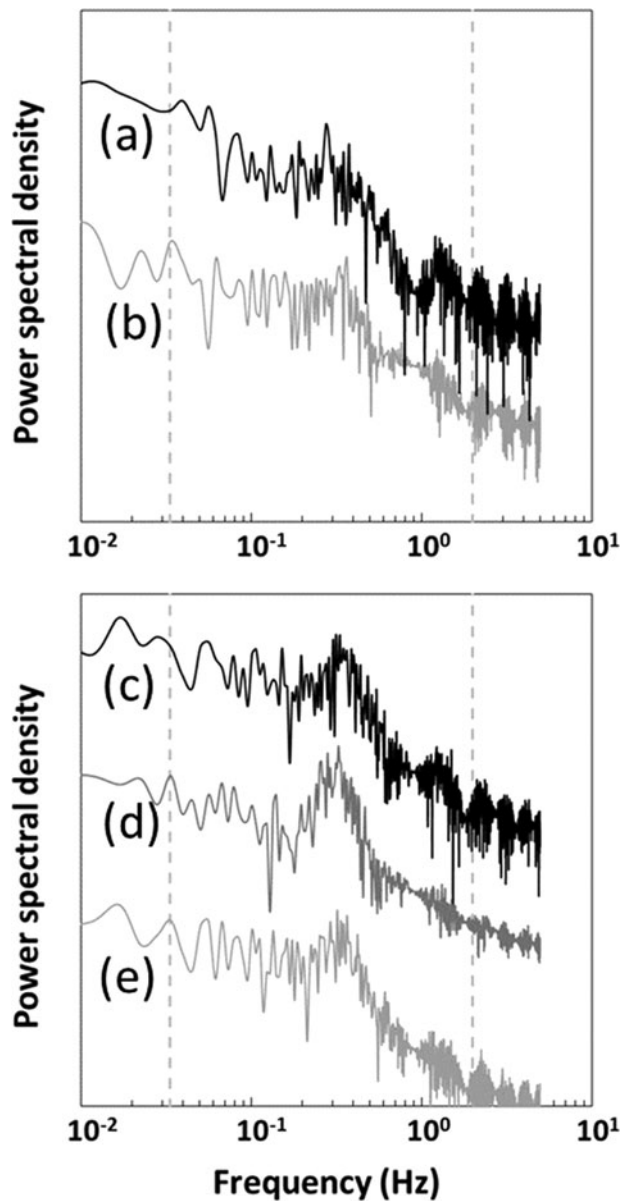


**Figure 6.** Power spectral density for 3-min bursts in 2008 for summer on (a) 8 August beginning at 1900 h and (b) 18 August beginning at 1700 h, and winter on (c) 9 December beginning at 0100 h, (d) 13 December beginning at 0700 h, and (e) 19 December beginning at 0900 h. The vertical dashed lines demarcate the so-called wind-wave band from 0.033 to 2 Hz (corresponding to wave periods between 0.5 and 30 s). Note that the spectra are offset for illustrative purposes.

for instances when bottom shear stress exceeded the critical shear stress, we observed the most energetic peak in the power spectral density plots at 0.28 Hz (Fig. 6a) and 0.37 Hz (Fig. 6b), corresponding to the wind-wave contribution from wave periods equal to 3.6 and 2.7 s, respectively. For high-wind events in winter, more pronounced peaks in power spectral density of 0.30–0.35 Hz were observed (Fig. 6c–e), correspond-

ing to the wind-wave contribution from wave periods of 2.9–3.3 s.

### Sediment characteristics

Generally, we found that the sediment at the study site was well-sorted, noncohesive, and with no apparent bedforms. We verified that the presence of organic material was negligible. In addition, we assumed that flocculation processes were negligible because specific conductivity was extremely low (typically  $<0.1 \mu\text{S}/\text{cm}$ ; D. Roberts, University of California, Davis, 2015, unpubl. data). Considering the grab samples collected at the study site, the lakebed sediment was about 92% sand, 7% silt, and  $<1\%$  clay (Wentworth 1922), consistent with a substrate map developed to assess fish habitat suitability by Herold et al. (2007), which showed a predominance of sand in the entire south shore of Lake Tahoe. We assumed a representative grain size of  $150 \mu\text{m}$ , corresponding to  $\sim d_{10}$  from the particle size distributions of the 2 grab samples (Reardon et al. 2014). Furthermore,  $150 \mu\text{m}$  corresponded to the peak in SSC by mass concentration during sediment resuspension events (Reardon et al. 2014). Following the formulation found in Parker (2004), the critical shear stress for incipient motion for a particle size of  $150 \mu\text{m}$  is 0.081 Pa.

### Sediment resuspension

For the summer study period, we observed a pattern of daily, elevated, midafternoon bottom shear stress (computed with the modified turbulent kinetic energy method; Reardon et al. 2014). At a water depth of 5 m, we observed 2 instances when the bottom shear stress exceeded the critical shear stress: 8 August 2008 (day 221) and 18 August 2008 (day 231; Fig. 4e). For the winter study period, we observed bottom shear stress that demonstrated no regular daily patterns; similar to the wind record, low measures were interrupted by abrupt increases (Fig. 5e). At a water depth of 5 m, we observed 3 instances where the bottom shear stress exceeded the critical shear stress: 8 December 2008 (days 343–344), 13 December 2008 (days 347–348), and 19 August 2008 (day 354; Fig. 5e).

For summer, the mean bottom shear stress over the study period ranged from 0.001 to 0.007 Pa. The maximum bottom shear stress was 0.093 Pa and associated with wind of southwesterly direction, the only wind

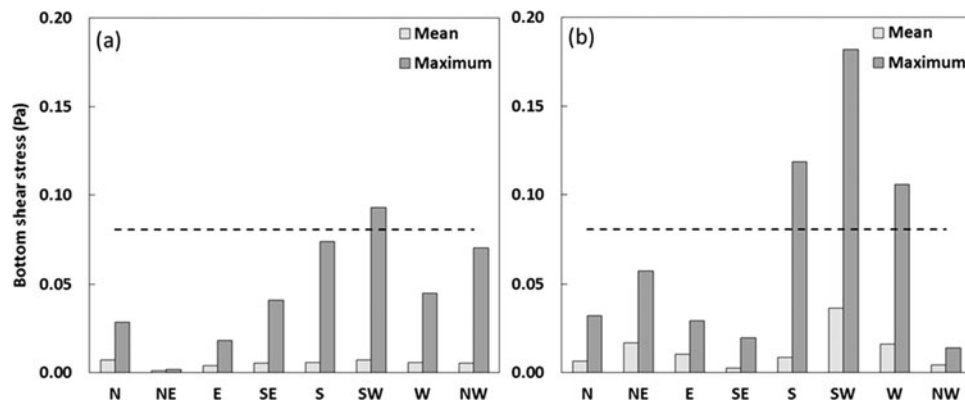


**Figure 7.** Mean and maximum bottom shear stress at a water depth of 5 m separated by wind direction for (a) summer and (b) winter. The horizontal dashed line at 0.081 Pa indicates the critical shear stress for incipient motion for a representative particle size of 150  $\mu\text{m}$ .

direction for which the bottom shear stress developed in excess of the critical shear stress (Fig. 7a). Generally, values of bottom shear stress were greater in winter than summer, attributed to greater wind intensity observed in winter. For winter, the mean bottom shear stress ranged from 0.003 to 0.036 Pa. The maximum bottom shear stress was 0.182 Pa and associated with wind of southwesterly direction; bottom shear stress also exceeded the critical shear for southerly (0.119 Pa) and westerly (0.106 Pa) wind directions (Fig. 7b). The wind directions associated with maximum bottom shear stress were the same wind directions as for the maximum observed wind speeds.

During winter we collected *in situ* measurements of SSC with an LISST-100X. We observed that SSC did not change with increasing total bottom shear stress for particles of median diameter 1.25–16  $\mu\text{m}$  (Fig. 8a). The Lake Tahoe TMDL attributes the loss of deep-water transparency, in part, to fine sediment (<16  $\mu\text{m}$ ). Furthermore, Swift et al. (2006) showed that particles

with the greatest potential to negatively impact lake clarity were inorganic and <10  $\mu\text{m}$ . Fine inorganic particles strongly scatter light, which results in decreased lake transparency (Davies-Colley and Smith 2001, Kirk 2011); however, we observed an increase in SSC for those instances when the bottom shear stress exceeded the critical shear stress for particles of median diameter 100–250  $\mu\text{m}$  (Fig. 8b).

#### Predictive tools developed from wind-wave modeling

The process of wind-driven nearshore sediment resuspension results in the entrainment of bed sediment into the water column, with wave height and water depth influencing the potential for resuspension (Fig. 9). Increasing wave heights resulted in increased bottom shear stress, leading to greater potential for resuspension; conversely, increasing water depth resulted in decreased bottom shear stress, leading to the diminished potential for resuspension. Considering

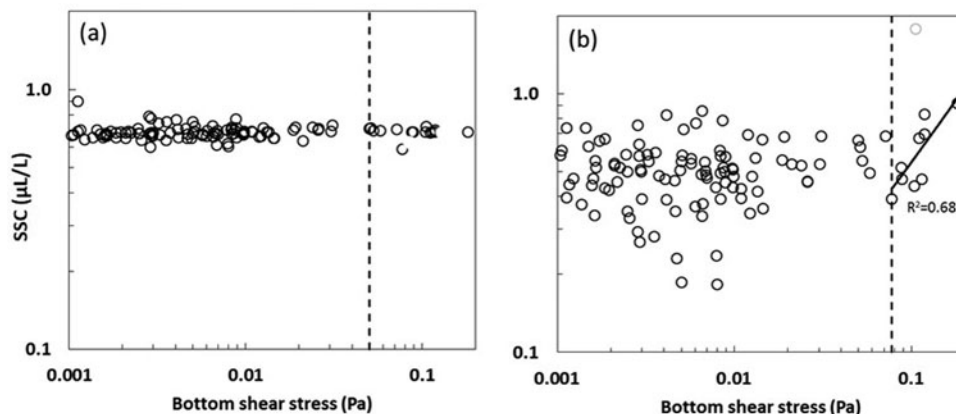


**Figure 8.** SSC vs. total bottom shear stress at a water depth of 5 m for particles of median diameter (a) 1.25–16  $\mu\text{m}$  and (b) 100–250  $\mu\text{m}$ . The vertical dashed line at (a) 0.050 Pa and (b) 0.077 Pa indicates the critical shear stress for incipient motion for a particle size of 1.25  $\mu\text{m}$  and 100  $\mu\text{m}$ , respectively (following Parker 2004). The data point indicated by the open gray circle was disregarded.

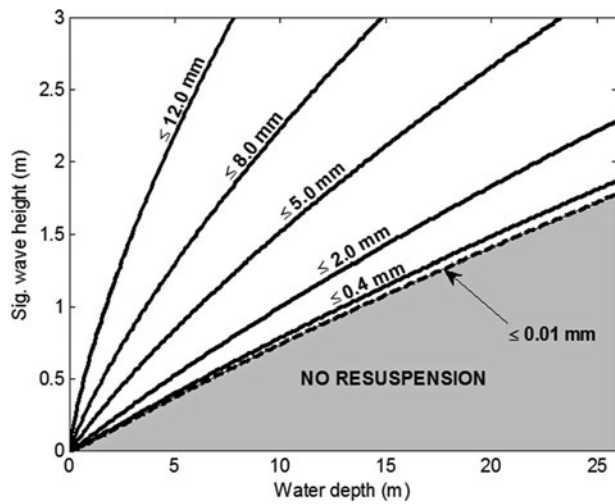


**Figure 9.** Particle resuspension with varying water depths and wave heights. Solid lines show the limit at which different particle diameters are resuspended from the lakebed. Similarly, the broken line shows the case for particles with diameter  $\leq 10 \mu\text{m}$ .

our representative grain size of  $150 \mu\text{m}$  and a maximum wave height of  $0.7 \text{ m}$ , the maximum water depth for which wind-driven surface waves may influence the lakebed sediment is  $9 \text{ m}$  (Fig. 9).

The potential for particle resuspension for 3 different water depths comes from the combination of wind speed and direction/fetch (Fig. 10). For the water depths shown, the greatest resuspension potential was achieved with the longest fetch, as expected. At the study site, the longest fetch ( $\sim 30 \text{ km}$ ) resulted from a northerly wind. The no-resuspension area (gray area) increased because the water depth was no longer shallow enough to favor the transfer of sufficient momentum of the wind-waves from the water surface to the sediment–water interface (Fig. 10).

Due to the complex bathymetry of the nearshore of Lake Tahoe, the relationship between lake level and the potential areal extent of wind-driven nearshore sediment resuspension is not linear. The areal extent of wind-driven nearshore sediment resuspension at Lake Tahoe's south nearshore zone changes with changing lake level (Fig. 11). For a lake level equal to the natural rim ( $1897 \text{ m}$ ), the potential area affected is  $8.3 \text{ km}^2$  (Fig. 11b); for a lake level equal to the maximum legal limit ( $1899 \text{ m}$ ), the potential area affected is  $7.2 \text{ km}^2$  (Fig. 11c); and finally, for a lake level equal to  $2 \text{ m}$  below the natural rim ( $1895 \text{ m}$ ), the potential area affected is  $4.7 \text{ km}^2$  (Fig. 11a). As the lake level drops below the natural rim, the potential areal extent of wind-driven nearshore sediment resuspension decreases (Fig. 11d) because with dropping lake

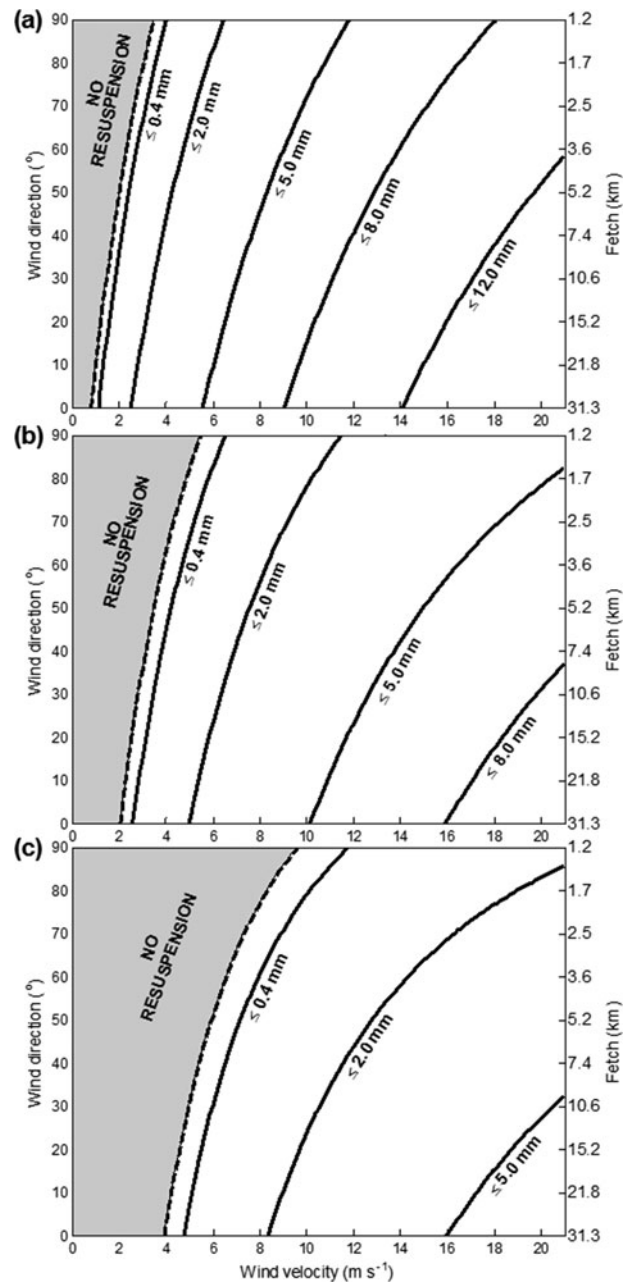


**Figure 10.** Resuspension curves considering different wind speed and direction for water depths of (a)  $2.1 \text{ m}$ , (b)  $4.2 \text{ m}$ , and (c)  $8.3 \text{ m}$ . The corresponding fetch is indicated on the secondary axis. Solid lines show the limit at which different particle diameters are resuspended from the lakebed. Similarly, the broken lines show the limiting case for particles with diameter  $\leq 10 \mu\text{m}$ .

level, the extent of the wetted area at Lake Tahoe decreases. As the lake level increases from the natural rim up to the maximum legal limit, the potential areal extent of wind-driven nearshore sediment resuspension also decreases (Fig. 11d) because as lake level increases, less of the nearshore is sufficiently shallow for the transfer of momentum of the wind-waves from the surface to the sediment–water interface. As a result,

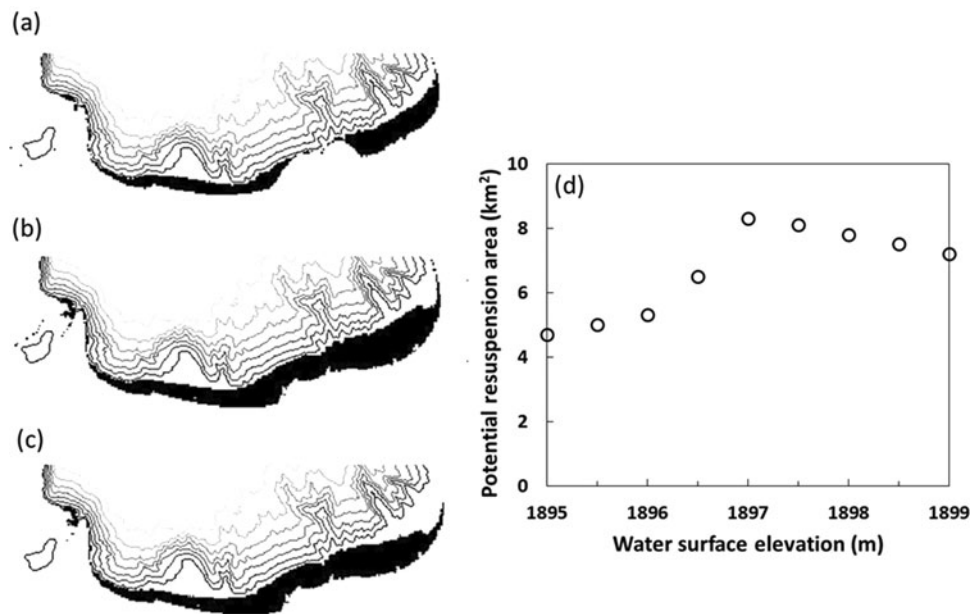


**Figure 11.** The areal extent of wind-driven sediment resuspension (denoted by black) in Lake Tahoe's southern nearshore zone, considering lake water level equal to (a) 2 m below the natural rim (1895 m), (b) the natural rim (1897 m), and (c) the maximum legal limit (1899 m). The area potentially affected by wind-driven sediment resuspension is (a) 4.7 km<sup>2</sup>, (b) 8.3 km<sup>2</sup>, and (c) 7.2 km<sup>2</sup>. Contours are shown at 50 m intervals. (d) Potential resuspension area with changing water surface elevation.

the potential for wind-driven sediment resuspension is reduced.

### Summary and conclusions

To elucidate the relationship between nearshore sediment resuspension and water clarity at Lake Tahoe over summer and winter, we synthesized field observations of hydrodynamic and sediment variables, computations of bottom shear stress, and simulations from previously modified and validated wind-wave model STWAVE. This paper reported the first comprehensive, process-based study of sediment resuspension at Lake Tahoe throughout the year, offering insight to others facing management challenges at deep, oligotrophic lakes.

In summer, we observed that the time series is characterized by a strong diurnal pattern with wind intensity peaking each day at mid-afternoon. By contrast, in winter we observed low-wind periods punctuated by high-energy storm events. Both low-wind and high-wind periods were sustained for days at a time with no regular pattern. Generally, the onset of wind events ended the thermal stratification of the water column within several hours. Based on these results, the thermal structure did not greatly impact the transfer of momentum in the water column.

Considering the nature of the wind-waves, we observed that the peak in the power spectral density plots corresponded to a wave period of about 3 s in both summer and winter. In summer, the form of the power spectral density plot is less pronounced than those for winter. In winter, we see strong peaks of similar form for each burst and attribute this to the greater wind intensity in winter and therefore the more evident differentiation of the high-frequency, nearbed velocity signal.

We considered wind conditions that may derive the maximum bottom shear stress and found that wind-driven surface waves resulted in potential sediment resuspension up to a water depth of 9 m. This influence extended to a lake area of 8.3 km<sup>2</sup> for a lake water level equal to the natural rim and decreased both as the lake water level increased to the maximum legal limit (7.2 km<sup>2</sup>) and decreased to 2 m below the natural rim (4.7 km<sup>2</sup>).

We determined that wind-waves do not greatly disturb the sediment-water interface at the study site (i.e., the south end of Lake Tahoe 1000 m offshore at a water depth of ~5 m). The processes we observed were subtle and nuanced compared to similar phenomena at shallow, wind-exposed lakes like the Salton Sea (Chung et al. 2009a, 2009b). With increasing bottom shear stress attributed to wind-waves, the SSC of particles

of median diameter 1.25–16  $\mu\text{m}$  did not change. For particles of median diameter 100–250  $\mu\text{m}$ , we saw an increase (same order of magnitude) in SSC for those instances when the bottom shear stress exceeded the critical shear stress. In general, we attribute the relative lack of fine material available for resuspension to the coarse and granular lakebed sediment at the nearshore of Lake Tahoe.

An important consideration is how these research findings can be translated to management strategies. The results suggested that wind-driven nearshore sediment resuspension does not produce an increase in particle loading of the size class identified to most negatively impact water clarity; however, the resuspension of coarser material has the potential to increase the internal loading of nutrients and contaminants from the lakebed. Alexander and Wigart (2013a, 2013b) demonstrated an association between the average daily increase in turbidity and high-intensity boating in the southern nearshore of Lake Tahoe. The authors attributed the decline in apparent water quality to resuspended sediment and released nutrients from boating-induced wave action and turbulence (Alexander and Wigart 2013a, 2013b). We recommend assessing the potential for internal loading of nutrients by both resuspension and hypolimnetic anoxia, which has not yet been investigated. In addition, it would be worthwhile to extend the geographic scope to include field measurements of wind-driven sediment resuspension from other nearshore areas of the lake, particularly to assess the availability of fine sediment.

### Acknowledgments

The Vector was provided as a Nortek 2008 Student Equipment Grant Award. The ADVOcean Probe was provided on loan from the US Geological Survey. The Western Regional Climate Center, Desert Research Institute, provided the meteorological data that was collected at the Timbercove station by TERC. We also wish to acknowledge key students and staff from the Environmental Dynamics Laboratory and TERC, both of the University of California, Davis. In particular, we thank Erik Maroney, an undergraduate at the University of California, Davis, for cleaning 10 yr of meteorological data.

### Funding

This research was supported by the University of California, Davis, and a grant from the US Department of Agriculture Forest Service Pacific Southwest Research Station using funds provided by the Bureau of Land Management through the sale of

public lands as authorized by the Southern Nevada Public Land Management Act.

### References

- Alexander MT, Wigart RC. 2013a. Effect of motorized watercraft on summer nearshore turbidity at Lake Tahoe, California-Nevada. *Lake Reserv Manage.* 29:247–256.
- Alexander MT, Wigart RC. 2013b. Effect of motorized watercraft on summer nearshore turbidity at Lake Tahoe, California-Nevada. *Lake Reserv Manage.* 29:256a–256b.
- Andrews S, Nover D, Schladow SG, Reuter JE. 2011. Limitations of laser diffraction for measuring fine particles in oligotrophic systems: pitfalls and potential solutions. *Water Resour Res.* 47:W05523.
- Bloesch J. 1994. A review of methods used to measure sediment resuspension. *Hydrobiologia.* 284:13–18.
- Bunya S, Dietrich JC, Westerink JJ, Ebersole BA, Smith JM, Atkinson JH, Jensen R, Resio DT, Luettich RA, Dawson C, et al. 2010. A high-resolution coupled riverine flow, tide, wind, wind wave, and storm surge model for southern Louisiana and Mississippi. Part I: Model development and validation. *Mon Weather Rev.* 138:345–377.
- California Regional Water Quality Control Board, Lahontan Region and Nevada Division of Environmental Protection. 2010. Lake Tahoe total maximum daily load technical report.
- Chung EG, Bombardelli FA, Schladow SG. 2009a. Sediment resuspension in a shallow lake. *Water Resour Res.* 45:W05422.
- Chung EG, Bombardelli FA, Schladow SG. 2009b. Modeling linkages between sediment resuspension and water quality in a shallow, eutrophic, wind-exposed lake. *Ecol Modell.* 220:1251–1265.
- Davies-Colley RJ, Smith DG. 2001. Turbidity, suspended sediment, and water clarity: a review. *J Am Water Resour Assoc.* 37:1085–1101.
- Dettinger MD. 2012. Projections and downscaling of 21st century temperatures, precipitation, radiative fluxes and winds for the Southwestern US, with focus on Lake Tahoe. *Climatic Change.* 116:17–33.
- Dietrich JC, Bunya S, Westerink JJ, Ebersole BA, Smith JM, Atkinson JH, Jensen R, Resio DT, Luettich RA, Dawson C, et al. 2010. A high-resolution coupled riverine flow, tide, wind, wind wave, and storm surge model for southern Louisiana and Mississippi. Part II: Synoptic description and analysis of hurricanes Katrina and Rita. *Mon Weather Rev.* 138:378–401.
- Evans RD. 1994. Empirical evidence of the importance of sediment resuspension in lakes. *Hydrobiologia.* 284:5–12.
- García MH. 2008. Sediment transport and morphodynamics. In: García MH, editor. *Sedimentation engineering: measurements, modeling and practice.* Reston (VA): ASCE Manual of Practice 110.
- Goldman CR. 1988. Primary productivity, nutrients, and transparency during the early onset of eutrophication in

- ultra-oligotrophic Lake Tahoe, California-Nevada. *Limnol Oceanogr.* 33:1321–1333.
- Håkanson L, Jansson M. 1983. *Principles of lake sedimentology*. Berlin (Germany): Springer-Verlag.
- Herold M, Metz J, Romsos JS. 2007. Inferring littoral substrates, fish habitats, and fish dynamics of Lake Tahoe using IKONOS data. *Can J Remote Sens.* 33: 445–456.
- Kamphuis JW. 1975. Friction factor under oscillatory waves. *J Waterw Harbors Coastal Eng Div.* 101:135–144.
- Kim SC, Friedrichs CT, Maa JPY, Wright LD. 2000. Estimating bottom stress in tidal boundary layer from acoustic Doppler velocimeter data. *J Hydraul Eng.* 126:399–406.
- Kirk JTO. 2011. *Light and photosynthesis in aquatic ecosystems*. 3rd ed. Cambridge (UK): University Press.
- Kundu PK, Cohen IM, Dowling DR. 2012. *Fluid mechanics*. 5th ed. San Diego (CA): Academic Press.
- Luetlich RA, Harleman DRF, Somlyódy L. 1990. Dynamic behavior of suspended sediment concentrations in a shallow lake perturbed by episodic wind events. *Limnol Oceanogr.* 35:1050–1067.
- Massey TC, Anderson ME, Smith JM, Gomez J, Jones R. 2011. *STWAVE: Steady-state spectral wave model user's manual for STWAVE*. Version 6.0. Vicksburg (MS): US Army Engineer Research and Development Center.
- Norrman JO. 1964. Lake Vättern: investigations on shore and bottom morphology. *Geogr Ann* 46:1–238.
- Parker G. 2004. *1D sediment transport morphodynamics with applications to rivers and turbidity currents*. Minneapolis (MN): National Center for Earth Surface Dynamics. E-book available from <http://cee.uiuc.edu/people/parkerg/>
- Raudkivi AJ. 1998. *Loose boundary hydraulics*. 3rd ed. Oxford (UK): Pergamon Press.
- Reardon KE, Bombardelli FA, Moreno-Casas PA, Rueda FJ, Schladow SG. 2014. Wind-driven nearshore sediment resuspension in a deep lake during winter. *Water Resour Res.* 50:8826–8844.
- Ren D. 2010. Effects of global warming on wind energy availability. *Renew Sustainable Energy Rev.* 2:052301.
- Sahoo GB, Schladow SG, Reuter JE, Coats R, Dettinger M, Riverson J, Wolfe B, Costa-Cabral M. 2012. The response of Lake Tahoe to climate change. *Climatic Change.* 116:71–95.
- Shields IA. 1936. *Anwendung der ahnlichkeitmechanik und der turbulenzforschung auf die gescheibebewegung*. Berlin (Germany): Mitt. Preuss Ver.-Anst.
- Swift TJ, Perez-Losada J, Schladow SG, Reuter JE, Jassby AD, Goldman CR. 2006. Water clarity modeling in Lake Tahoe: linking suspended matter characteristics to Secchi depth. *Aquat Sci.* 68:1–15.
- [UCD TERC] University of California, Davis Tahoe Environmental Research Center. 2015. *Tahoe: State of the Lake Report 2015*.
- Wentworth CK. 1922. A scale of grade and class terms for clastic sediments. *J Geology.* 30:377–392.